Stochastic Forcing of Small-Amplitude Oscillations in the Stratosphere

ROLANDO R. GARCIA AND JOHN E. GEISLER[1]

National Center for Atmospheric Research,[2] Boulder, CO 80307

(Manuscript received 12 March 1981, in final form 11 May 1981)

ABSTRACT

A quasi-geostrophic β-plane channel model is used to study the response of the stratosphere to planetary waves forced at the ground. The forcing consists of a standing field of eddy vertical velocity whose amplitude fluctuates randomly about a time-average value. Cross-spectrum analysis of model results reveals the presence of westward traveling waves and, among these, of normal modes in the model solution. The superposition of the traveling waves and a stationary wave maintained by the time-average forcing gives rise to oscillating eddy heat fluxes. The relationship of these fluxes to changes in the zonal-mean temperature gradient is investigated by means of the squared coherence statistic. We examine how the occurrence of high levels of coherence depends on the existence of the external normal mode and on the presence of noise introduced into the model output.

1. Introduction

Quasi-periodic fluctuations on a time scale of the order of two weeks in the mean and eddy fields of the wintertime stratosphere have been reported by various authors in the last two decades. Muench (1965) found evidence for periodic amplifications in wavenumbers 1 and 2 up to 10 mb in the Northern Hemisphere winter; Finger *et al.* (1966), using rocket data from 5 to 0.4 mb, observed oscillations in the heights of constant pressure surfaces in the upper stratosphere; and Hirota and Sato (1969) reported a periodicity of about two weeks in both the strength of the polar night vortex and the amplitude of wavenumber 1 at 30 mb. Hirota and Sato further noted that the oscillations in zonal wind and wave amplitude were negatively correlated.

More recent studies have revealed quasi-periodic behavior in tropospheric and stratospheric energy cycles (Miller, 1974); in the zonal index, momentum flux and kinetic energy of the upper troposphere (Webster and Keller, 1975); and in the zonal mean temperature and the amplitudes of waves 1 and 2 (van Loon *et al.*, 1975). The study of Webster and Keller used Southern Hemisphere data, as did studies by Harwood (1975) and Leovy and Webster (1976), thus indicating that the occurrence of quasi-periodic oscillations in the wintertime stratosphere is not limited to the Northern Hemisphere.

Madden (1975) has interpreted the observations of van Loon *et al.* in terms of fluctuating eddy heat fluxes that give rise to corresponding changes in the zonal mean temperatures. The fluctuations in the eddy heat fluxes are ascribed to the modulation of a forced, stationary wave by transient waves. The latter, Madden argues, could be identified with theoretically predicted normal modes of the atmosphere, excited by variations in the mean tropospheric zonal wind whose spectrum is that of red noise. Although the mechanism proposed by Madden was offered specifically as an explanation for the results reported by van Loon *et al.* it could also serve to explain the findings of at least some of the other studies cited above.

Few theoretical investigations have been carried out to test this or any other mechanism that might be responsible for the observed stratospheric oscillations. Hirota (1971), used a quasi-geostrophic β-plane model in which a traveling wave, excited by periodic changes about a mean value in the tropospheric zonal wind, is superimposed on a steady, stationary wave. The result is an oscillation of the wave amplitudes in both the model troposphere and stratosphere. Although Hirota's model is consistent in some respects with observations, it has the shortcoming that the zonal wind is prescribed and therefore cannot change in response to time-varying wave forcing. Holton and Mass (1976) have used a model in which both the eddies and mean wind are predicted and can interact with each other. Waves in the model are forced by specifying the eddy geopotential height at the tropopause. Although this model can produce oscillations in both

[1] Permanent affiliation: Rosenstiel School of Marine and Atmospheric Sciences, University of Miami, 4600 Rickenbacker Causeway, Miami, FL 33149.

[2] The National Center for Atmospheric Research is sponsored by the National Science Foundation.

0022-4928/81/102187-11$06.75

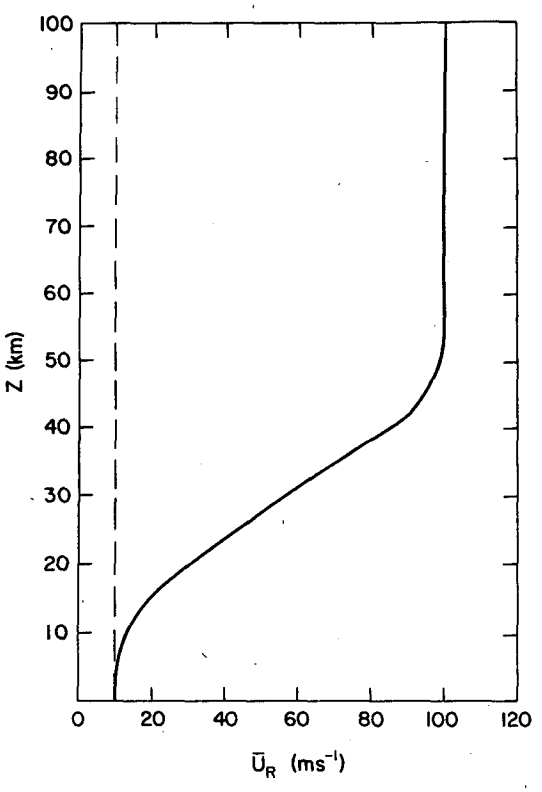

FIG. 1. The radiative equilibrium zonal wind profile u_R at model equinox (dashed line) and model solstice (solid line).

wave amplitude and zonal wind velocity, these oscillations are essentially a succession of sudden warming episodes. A buildup of wave amplitude leads to a reversal of the zonal wind which, in turn, inhibits the vertical propagation of the waves. The wind then becomes westerly once again through radiative relaxation, and the cycle starts anew. The period of the oscillations decreases with increasing strength of the forcing at the lower boundary but, in general, is rather longer than two weeks except for very strong forcing. A number of authors (Geisler and Dickinson, 1976; Schoeberl and Clark, 1980; Salby, 1981) have modeled the structure of Rossby normal modes in spherical geometry under a variety of realistic zonal mean state configurations. These works, however, do not address the question of how the modes are excited or what effect they have on the zonal mean state.

In the present study we investigate, with a simple model, the mechanism for small-amplitude stratospheric oscillations proposed by Madden. We use a quasi-geostrophic model formulated on a β plane, and study the evolution of the zonal mean state in response to wave forcing as well as the evolution of the waves themselves. The waves in our model are forced by a standing eddy vertical velocity field at the ground whose amplitude varies about some mean value. No periodicity is assumed for these variations; instead, they are taken to be random fluctuations with a red noise spectrum. When the model is forced in this way, waves are produced whose amplitude appears to oscillate regularly. We analyze the spectrum of wave response in the stratosphere and identify normal modes that are present. Following Madden's analysis of observations, we calculate the squared coherence between eddy heat flux and the zonally averaged temperature gradient across the β-plane channel and elucidate the factors affecting this coherence.

2. The numerical model

We assume quasi-geostrophic dynamics on a β-plane centered at 60° latitude and extending from 30 to 90°. The governing equations are the same as those used by Holton and Mass (1976). The eddies obey a linearized potential vorticity equation for the streamfunction ψ'

$$\left(\frac{\partial}{\partial t}+\bar{u}\frac{\partial}{\partial x}\right)\left[\nabla^2\psi'+\frac{f_0^2}{N^2}\frac{1}{\rho_s}\frac{\partial}{\partial z}\left(\rho_s\frac{\partial\psi'}{\partial z}\right)\right]+\beta_e\frac{\partial\psi'}{\partial x}+\frac{f_0^2}{N^2}\frac{1}{\rho_s}\frac{\partial}{\partial z}\left(\rho_s\alpha\frac{\partial\psi'}{\partial z}\right)=0, \quad (1)$$

where

$$\beta_e=\beta-\frac{\partial^2\bar{u}}{\partial y^2}-\frac{f_0^2}{N^2}\frac{1}{\rho_s}\frac{\partial}{\partial z}\left(\rho_s\frac{\partial\bar{u}}{\partial z}\right)$$

is the effective gradient of potential vorticity, f_0 is the Coriolis parameter at 60° latitude, $z=-H\ln(p/p_0)$ is the height in log-pressure coordinates, and $\rho_s=\rho_0\times\exp(-z/H)$. The scale height H of the log-pressure coordinate system is set to 7 km. N^2 is the square of the buoyancy frequency, taken to be equal to the constant value 4×10^{-4} s^{-2}. Finally, α is a Newtonian cooling coefficient whose vertical dependence is taken from Dickinson (1973).

The zonal mean state obeys the following set of equations:

$$\frac{\partial\bar{u}}{\partial t}-f_0\bar{v}=-\frac{\partial\overline{u'v'}}{\partial y}, \quad (2)$$

$$\frac{\partial\bar{T}}{\partial t}+\frac{HN^2}{R}\bar{w}=-\frac{\partial\overline{v'T'}}{\partial y}-\alpha(\bar{T}-\bar{T}_R), \quad (3)$$

$$\frac{\partial\bar{v}}{\partial y}+\frac{1}{\rho_s}\frac{\partial}{\partial z}(\rho_s\bar{w})=0, \quad (4)$$

where $\bar{T}_R$ is a radiative equilibrium temperature, and the zonal mean wind and temperature are in thermal wind balance:

$$\frac{\partial\bar{u}}{\partial z}=-\frac{R}{f_0H}\frac{\partial\bar{T}}{\partial y}. \quad (5)$$

Eqs. (2)–(4) can be combined with the aid of (5)

to give a predictive equation for the zonal wind:

$$\frac{\partial}{\partial t}\left[\frac{\partial^2 \bar{u}}{\partial y^2} + \frac{f_0^2}{N^2}\frac{1}{\rho_s}\frac{\partial}{\partial z}\left(\rho_s \frac{\partial \bar{u}}{\partial z}\right)\right] = -\frac{f_0^2}{N^2}\frac{1}{\rho_s}\frac{\partial}{\partial z}\left[\rho_s \alpha\left(\frac{\partial \bar{u}}{\partial z} - \frac{\partial \bar{u}_R}{\partial z}\right)\right] + \frac{f_0}{N^2}\frac{R}{H}\frac{\partial^2}{\partial y^2}\left[\frac{1}{\rho_s}\frac{\partial}{\partial z}(\rho_s \overline{v'T'})\right], \quad (6)$$

where $\bar{u}_R$ is in thermal wind balance with the radiative equilibrium temperature $\bar{T}_R$. We are interested in modeling the response of the stratosphere to wave forcing over the half year centered about the winter solstice. Accordingly, we let $\bar{u}_R$ be given by

$$\bar{u}_R(z,t) = u_0 + (\Delta u/2)\cdot\left[1 + \tanh\left(\frac{z-35}{12.6}\right)\right]\cdot F(t), \quad (7)$$

where $u_0 = 10$ m s^{-1}, $\Delta u = 90$ m s^{-1}, z is log-pressure height in kilometers, and $F(t)$ specifies a semi-annual cycle

$$F(t) = \tfrac{1}{2}\left[1 - \cos\left(\frac{2\pi t}{180}\right)\right] \quad (8)$$

with t in days. The resulting profile of $\bar{u}_R$ is shown in Fig. 1 for model equinox ($t = 0$, 180 days) and model solstice ($t = 90$ days).

Eqs. (1) and (6) together predict the development of the zonal mean state, represented by $\bar{u}$, and the perturbations to this state, represented by the eddy streamfunction ψ'. To solve these equations, we assume the following forms for $\bar{u}$ and ψ':

$$\left.\begin{aligned}\bar{u} &= U(z,t)\sin ly \\ \psi' &= \psi(z,t)e^{z/2H}e^{ikx}\sin ly\end{aligned}\right\}. \quad (9)$$

In (9), k is the zonal wavenumber and $l = 3/a$, where a is the radius of the Earth. The choice of l implies a meridional structure for both ψ' and $\bar{u}$ which has a maximum at the center of the β-plane channel and decays to zero at the northern and southern boundaries. When the forms (9) are substituted into (1) and (6), equations can be derived for $U(z,t)$ and $\psi(z,t)$. The reader is referred to Holton and Mass (1976) for the details of the derivation. We use a vertical resolution of 2 km and a time step of 1 h in all model runs.

We require as boundary conditions that $\bar{w} = 0$ at the top ($z = 100$ km) and bottom ($z = 0$) of the model. Note that, in general, the boundary condition at the ground in the presence of topography is $\bar{w} = \overline{(v'h')}y$ (McIntyre, 1980). However, in the present model $\overline{v'h'} = -(k\bar{u}/g)\,\mathrm{Im}(\psi'\psi'_y{}^*) = 0$ because ψ' has no phase variation across the β-plane channel. The eddy vertical velocity is also assumed to vanish at the top, but is specified at the lower boundary. The eddy vertical velocity in geometric coordinates w' is related to the streamfunction ψ' by the equation

$$\left(\frac{\partial}{\partial t} + \alpha + \bar{u}\frac{\partial}{\partial x}\right)\frac{\partial \psi'}{\partial z} - \frac{N^2}{g}\frac{\partial \psi'}{\partial t} - \frac{\partial \bar{u}}{\partial z}\frac{\partial \psi'}{\partial x} = -\frac{N^2 w'}{f_0}. \quad (10)$$

By specifying w' in Eq. (10) it is possible to force waves whose development is governed by (1) and which can interact with the zonal mean state according to (6). We let w' be of the form

$$w' = w(t)e^{ikx}\sin ly,$$

where $w(t)$ is composed of two parts:

$$w(t) = w_E(t) + w_F(t).$$

Here w_F is a prescribed forcing and w_E represents frictional dissipation in the boundary layer, parameterized as Ekman pumping, i.e.,

$$w_E = -\frac{1}{2}\left(\frac{2K}{f_0}\right)^{1/2}\nabla^2\psi', \quad (11)$$

where K is an eddy viscosity coefficient, which we take as 10^5 cm^2 s^{-1}.

In constructing an expression for w_F we assume

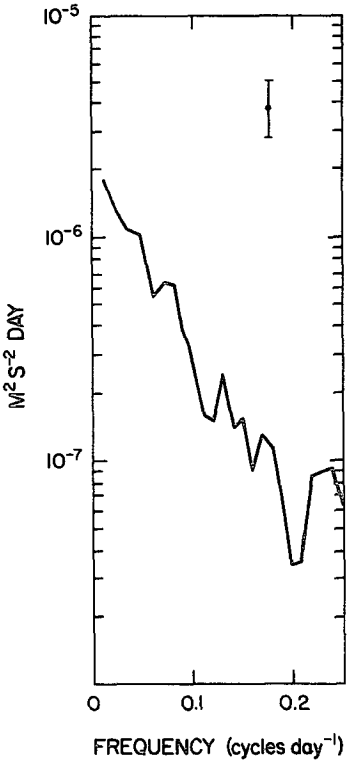

FIG. 2. Power spectrum of the eddy vertical velocity field at the lower boundary. The mean has been removed before computing the spectrum. Error bar denotes 99% confidence limits.

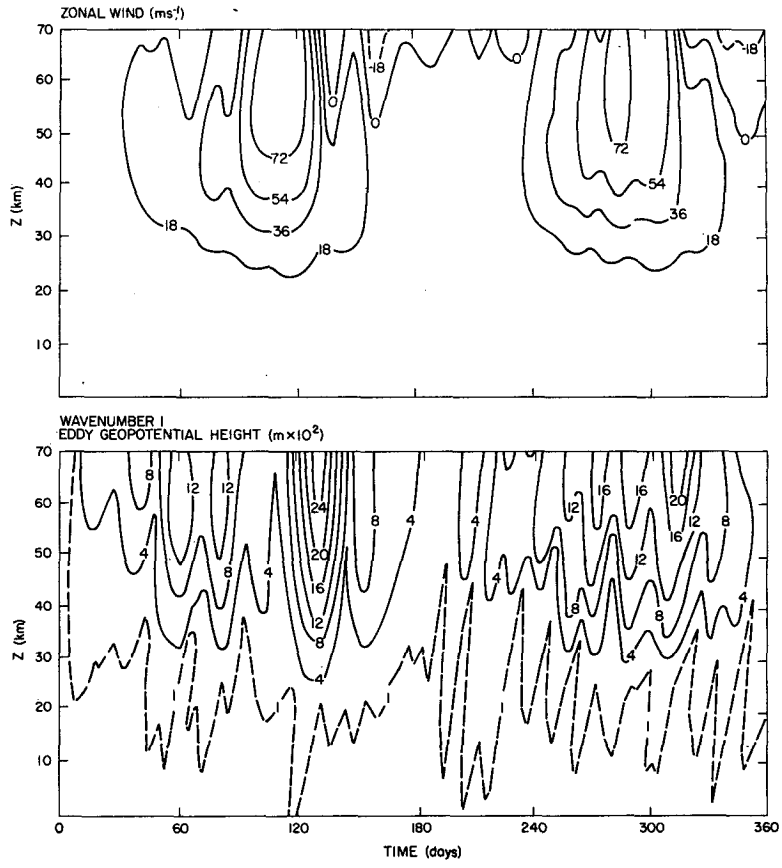

FIG. 3. Zonally averaged wind and wave number 1 geopotential heights for two model "seasons". Winter solstices occur at 90 and 270 days; equinoxes at 0, 180 and 360 days.

only that this vertical velocity can be represented as a first-order autoregressive process

$$w_F(t + \tau) = Rw_F(t) + \epsilon(t) + (1 - R)\langle w_F \rangle, \quad (12)$$

where $\langle w_F \rangle$ is the time mean of w_F, ϵ is a normally distributed random deviate of mean zero and variance σ^2, and R is the lag-τ autocorrelation coefficient. We pick a value for R by supposing that w_F is the result of a zonal wind blowing over topography h. Then

$$w_F = \bar{u} \frac{\partial h}{\partial x}, \quad (13)$$

and the autocorrelation coefficient is the same for w_F as it is for $\bar{u}$. Madden (1975) shows spectra for $\bar{u}$ at 60°N computed from data for eight winter seasons in the Northern Hemisphere. If one fits Madden's spectrum for 850 mb with the theoretical curve for the spectral power density of red noise (see, e.g., Gilman *et al.*, 1963), the value of R comes out to be ~0.79 for lag $\tau = 1$ day. The remaining parameters in (12) are chosen as follows: $\langle w_F \rangle$ is adjusted so that the model produces wave amplitudes in the stratosphere which are consistent with observations. We find that a value of 0.05 cm s^{-1} for $\langle w_F \rangle$ will give maximum eddy geopotential heights of ~2000 m at 60 km. If $\bar{u}$ is 10 m s^{-1} in the lowest layer of the model, our choice of $\langle w_F \rangle$ implies a wavenumber 1 topography of ~160 m at 60°N according to (13). While this is of the right order of magnitude, it is smaller than the actual value by a factor of 3 to 4. However, larger values of h (hence, of $\langle w_F \rangle$) lead to unrealistically large wave amplitudes in the model. The great sensitivity to wave forcing of the zonal mean state is characteristic of β-plane channel models like the present one (Holton and Dunkerton, 1978), but it should not detract from the qualitative validity of the results. Finally, the variance σ^2 of the random component of w_F is chosen in such a way that the ratio of the standard deviation of w_F to the mean of w_F is the same as the observed ratio of the standard deviation of $\bar{u}$ to the mean of $\bar{u}$.

The spectrum of the time-dependent forcing function w_F constructed by the procedure outlined above is shown in Fig. 2.

3. Results

a. Cross-spectrum analysis

The model is run starting from an undisturbed state wherein $\psi' = 0$ and $\bar{u} = \bar{u}_R$. At $t = 0$, the forcing function at the lower boundary (12) and the seasonal cycle of $\bar{u}_R$ (8) are turned on, and the model is allowed to run for five consecutive seasons to produce an ensemble of "observations" for spectral analysis. Fig. 3 shows the development of the zonal wind and the wavenumber 1 eddy geopotential heights for two model seasons. The seasonal cycle and, superimposed on it, oscillations in the amplitudes of both the zonal wind and eddy heights are easily noticeable. The latter appear to show some regularity, which is remarkable in view of the fact that the spectrum of the forcing function (Fig. 2) is red. Similar results (not shown) are obtained when the model is forced with a wavenumber 2 perturbation, but our discussion in the remainder of this paper will concentrate on wavenumber 1.

To investigate further the nature of the oscillations shown in Fig. 3, we apply the cross-spectrum analysis method described by Hayashi (1971) to the eddy streamfunction ψ' which is proportional to the height field. The method of Hayashi is able to resolve progressive (eastward moving) and retrogressive (westward moving) traveling waves present in the time series analyzed. The procedure used for estimating the cross spectrum (and all other spectral estimates presented in this paper) is similar to that outlined by van Loon *et al.* (1975). The mean of the time series is removed, and the first and last 10% of the series are tapered with a cosine curve to the average value of the first and last members of the series. The fast Fourier transform is then used to determine $N/2 + 1$ harmonic coefficients, where N is the number of members in the time series. Cross spectra are computed from the harmonic coefficients for each of the five model seasons, and these are averaged to give a smoothed estimate of the cross spectrum for the entire set of "data". This cross spectrum is smoothed further by taking a 1-2-1 running average in frequency. For the purpose of computing confidence limits, this procedure yields approximately 26 degrees of freedom (Jenkins and Watts, 1968, Chap. 6). Our method of determining spectral estimates differs from that used in van Loon *et al.* and in two recent papers by Madden (1975, 1978) in one respect. These authors taper the first and last 10% of the time series under analysis to zero after removing the mean. We show in the Appendix that this operation can seriously bias the spectral estimates in some instances.

The results of the cross-spectrum analysis of ψ' at the 24 km (30 mb) level of the model are shown in Fig. 4 for two cases. The solid curve shows the cross spectrum when the model is run with no Ekman layer [$K = 0$ in Eq. (11)], while the dashed curve is derived from a model run for which K was set to 10^5 cm^2 s^{-1}. Both spectra show a large amount of power associated with retrogressive traveling waves, and three peaks are apparent in the cross spectrum of the inviscid case. These correspond to the external (Lamb) normal mode, and to the first and second internal normal modes of our model. In the run with an Ekman layer present, the amplitude of the peak corresponding to the external mode is reduced substantially.

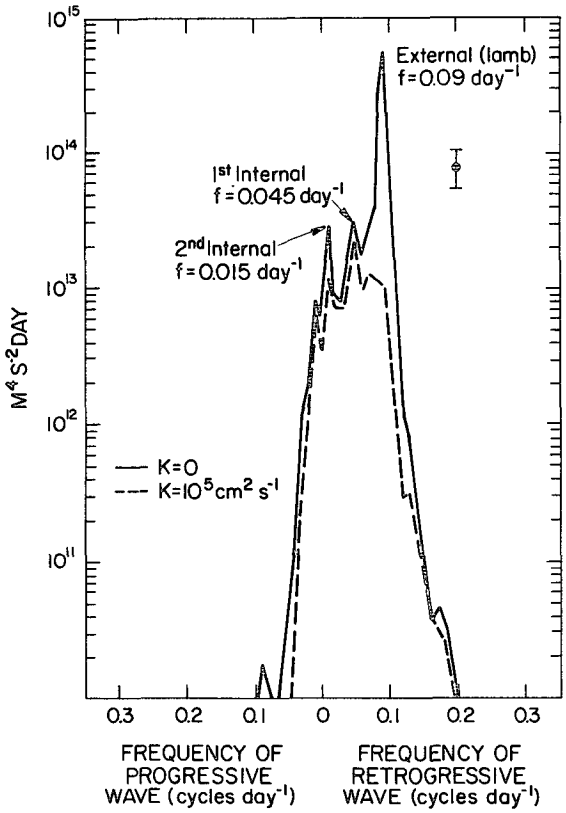

FIG. 4. Cross-spectrum of the eddy streamfunction at the 24 km (30 mb) level of the model. The dashed curve is for a run with an Ekman layer having an eddy diffusion coefficient of 10^5 cm^2 s^{-1}. The solid curve is the result of an inviscid run. In both cases, the mean was removed before computing the spectrum. The error bar shows the 99% confidence limits.

We base our identification of the peaks in the cross spectrum of Fig. 4 with retrogressive normal modes on a determination of the wave vertical structure at the center frequency of each of the peaks. This can be achieved easily because the cross-spectral analysis technique allows one to infer the amplitude and phase of traveling waves if one performs the analysis for all model levels at a given frequency (see Hayashi, 1971, for details). Fig. 5

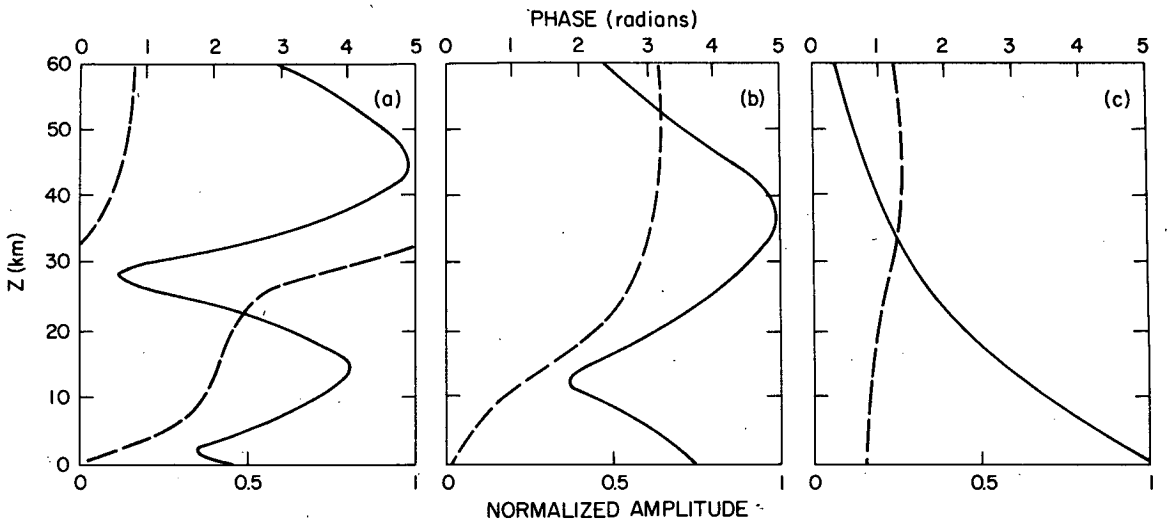

FIG. 5. Vertical structures of retrogressive traveling waves at (a) 0.015 day^{-1}, (b) 0.045 day^{-1} and (c) 0.09 day^{-1}. Amplitudes are normalized to unity.

shows vertical structures for frequencies of 0.015, 0.045 and 0.09 day^{-1}, which correspond to the peaks in Fig. 4. It is evident that these structures are those of two internal and an external mode, respectively. The properties of normal modes in β-plane channel models have been studied in detail by Geisler and Dickinson (1975). They find that, in addition to the external mode, internal free modes can exist if wave trapping occurs, i.e., if the solution to (1) becomes evanescent at some altitude where the westerly zonal wind is sufficiently strong. It should be noted that, strictly speaking, normal modes are eigensolutions of a linearized wave equation with constant coefficients (i.e., with a constant basic state). However, the term normal mode also has been used in a number of studies when trying to identify traveling planetary waves observed in the atmosphere with the results of analytical or numerical solutions of the linearized perturbation equations in spherical geometry. We follow this practice here since it appears that our model (and, by inference, the atmosphere) can respond preferentially to forcing at certain frequencies even when the zonal mean state is changing with time.

In view of the foregoing results, we conclude that the fluctuating amplitude of the eddy height field shown in Fig. 3 is produced mainly by the superposition of westward traveling waves and a stationary wave forced by the standing vertical velocity field at the lower boundary. The traveling waves are excited by the random variations in the strength of this vertical velocity field specified by Eq. (12).

We turn now to the question of oscillations in the zonal mean state, as evidenced by the evolution of the zonal wind shown in Fig. 3. The superposition of traveling and standing waves should give rise to oscillating eddy fluxes, and these fluxes should in turn force oscillations in zonal mean fields. Madden (1975) tested this hypothesis by examining the squared coherence between the eddy heat flux and the zonal mean temperature difference between middle and high latitudes. In what follows, we attempt to reproduce Madden's results by time series analysis of our model output, and we examine in detail the circumstances under which one might expect to obtain significant levels of squared coherence between eddy and zonal mean quantities.

b. *Coherence analysis*

The squared coherence and phase between two time series provides a measure of the correlation between these time series as a function of frequency. The squared coherence between $x(t)$ and $y(t)$ at frequency ω is defined by

$$\mathrm{Coh}_{xy}^2(\omega) = \frac{K_{xy}^2(\omega) + Q_{xy}^2(\omega)}{P_x(\omega)P_y(\omega)}, \qquad (13)$$

and the phase between these time series is

$$\phi_{xy}(\omega) = \tan^{-1}[Q_{xy}(\omega)/K_{xy}(\omega)]. \qquad (14)$$

In (13) and (14) K_{xy} and Q_{xy} are the cospectrum and quadrature spectrum of $x(t)$ and $y(t)$, respectively. P_x is the power spectrum of $x(t)$ and P_y, the power spectrum of $y(t)$. If $x(t)$ and $y(t)$ are strongly correlated and in phase (90° out of phase), $K_{xy}(Q_{xy})$ will be large and Coh_{xy}^2 will likewise be large. If $x(t)$ and $y(t)$ are not strongly correlated, both K_{xy} and Q_{xy} will be small, and so will Coh_{xy}^2. The phase statistic ϕ_{xy} will tend to zero if $x(t)$ and $y(t)$ are in phase (K_{xy} large, Q_{xy} small), and to $\pm 90°$ if $x(t)$ and $y(t)$ are out of phase (K_{xy} small, Q_{xy} large).

Madden (1975) made use of the squared coherence and phase statistics to determine the relationship between the time series of zonal mean temperature difference between high (70–80°N) and middle (40–50°N) latitudes and eddy heat transport across 60°N. The results of this analysis, which was based on data for eight winter seasons at the 30 mb pressure level are shown in Fig. 6. From these results, Madden concluded that fluctuations in the temperature difference and the eddy heat flux were coherent and in quadrature, with the heat flux leading, over a relatively wide band of frequencies. He went on to show that in the 1–3 week period range, a large fraction of the observed fluctuations in heat flux can be accounted for by the superposition of stationary and traveling planetary-scale waves.

We can carry out an analysis similar to Madden's by computing the squared coherence between the heat flux at the center of our β-plane channel and the zonal mean temperature gradient across the channel. The spectral estimates needed to construct the coherence and phase statistics (13)–(14) are obtained by the procedure described earlier in this section. However, before computing these spectral estimates we have added a certain amount of white noise to the time series of heat flux and mean temperature gradient produced by the model. We define the noise level as a given percentage of the mean of the time series in question. The addition of noise to the model output is intended to simulate the uncertainty associated with the measurement of the corresponding variables in the atmosphere. We will show below that the presence of noise in the data can have an important effect on the squared coherence.

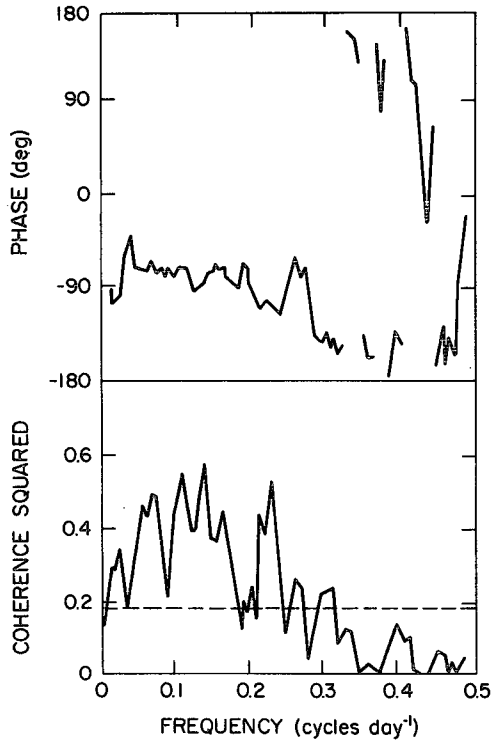

FIG. 6. The squared coherence between eddy heat flux and high-middle latitude temperature difference for eight Northern Hemisphere winters (Madden, 1975). Dashed line is the 99% confidence limit.

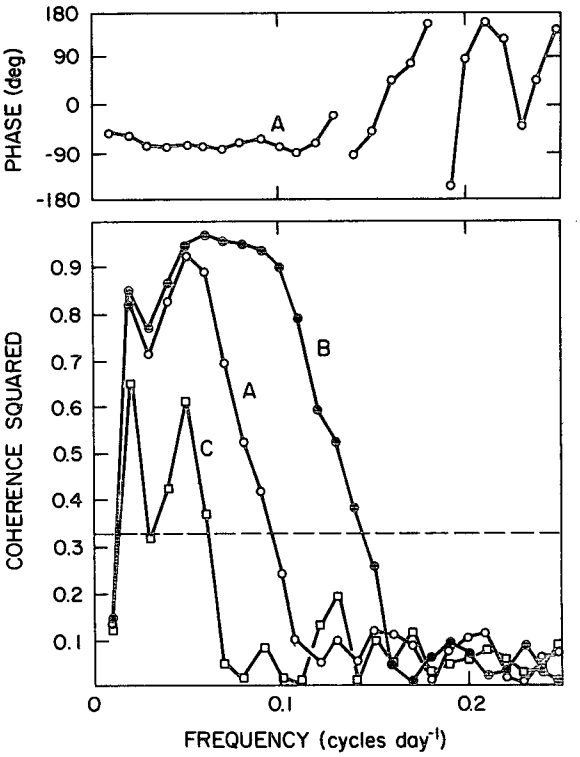

FIG. 7. Squared coherence (lower panel) between zonal mean temperature gradient and eddy heat flux computed from five model seasons after the addition of (A) 5%, (B) 1% and (C) 10% white noise to the time series. The phase statistic is also shown (upper panel) for the case with 5% white noise. Dashed line is the 99% confidence limit.

The squared coherence between the eddy heat flux and temperature gradient at the 24 km (30 mb) level of the model is shown in Fig. 7 for a run which includes an Ekman layer with $K = 10^5$ cm^2 s^{-1}. The three curves shown in the lower panel of the figure were obtained by analyzing the model output after adding different levels of noise (5% for curve A, 1% for B, and 10% for C). The 99% confidence limit, computed according to the formula given by Julian (1975) with 26 degrees of freedom, is denoted by the dashed line. For the sake of clarity, the phase statistic is shown in the upper panel of Fig. 7 only for the case with 5% added noise. The band of frequencies where the coherence is high corresponds roughly with that portion of the cross spectrum of ψ' (Fig. 4) which shows large amounts of power associated with traveling waves. However, the over-

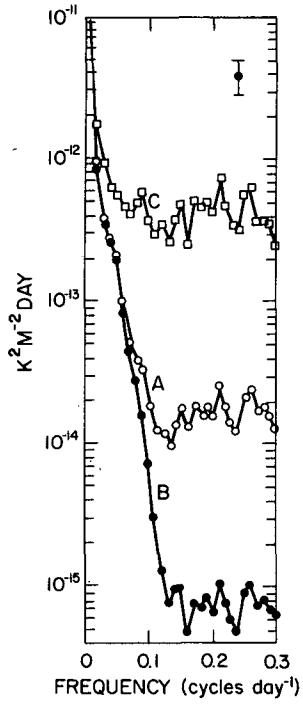

FIG. 8. Spectra of zonal mean temperature gradient computed from five model seasons after the addition of (A) 5%, (B) 1% and (C) 10% white noise. Error bar shows the 99% confidence limits.

all level of coherence within this band, and the drop in coherence at the higher frequencies is seen to be strongly dependent on the amount of noise added to the model output. When the noise level is 1%, significant levels of coherence are obtained at frequencies as high as 0.15 day^{-1}; but when the noise level is 10%, coherences are not significant beyond 0.07 day^{-1}.

To understand how noise in the model output can affect the computed coherence, we turn to Fig. 8. This figure shows the power spectrum of the zonal mean temperature gradient. Spectral power drops steeply from a high value at low frequencies until it levels off at a frequency which depends on the amount of noise added to the time series of mean temperature gradient. Above this frequency, the power of the noise is greater than the power of the temperature gradient "signal." Similar results are obtained for the spectrum of eddy heat flux (not shown). Since the white noise added to the time series of temperature gradient is not correlated with that added to the time series of eddy heat flux, it is clear that the drop in coherence at high frequencies seen in Fig. 7 is caused by the presence of noise. Within the band of frequencies where coherences are high, the power level of the noise is always smaller than that of the signal. Coherences in this band stay at significant levels, although their value drops as more noise is added to the model output.

The situation at very low frequency is somewhat different. Low coherence in this area is apparently due to the fact that, on this time scale, the temperature gradient is responding mainly to the seasonal-cycle forcing rather than to the eddy heat flux. Examination of the squared coherence between the temperature gradient and the seasonal-cycle forcing (not shown) does indeed reveal high levels of coherence between these time series at low frequencies.

For the purpose of comparing the results just presented with those obtained by Madden (1975), we note that the addition of 5% noise to our model output produces a spectrum of zonal mean temperature gradient whose shape resembles the spectra shown in Madden's paper. Comparison of Fig. 6 with curves A of Fig. 7 shows that our square coherence and phase statistics behave similarly to Madden's. The coherence is low at very low and at high frequencies, with a broad band of high coherence in between. Corresponding to the latter, there is a band of frequencies where the phase statistic is relatively constant and equal to $-90°$, which implies that the eddy heat flux leads the zonal mean temperature gradient. Our results thus lend support to Madden's conclusion that the superposition of stationary and traveling planetary waves produce oscillating heat fluxes which are capable of forcing oscillations in the zonal mean temperature gradient.

Our results also demonstrate that the existence of high squared coherence levels between two time series depends on the ratio of signal to noise in the time series. We obtain high coherence values at those frequencies where traveling waves have enough amplitude that they give rise to oscillating heat fluxes which are large compared to the noise introduced into the time series of heat flux. Turning again to the cross spectrum of ψ' shown in Fig. 4, we note that there are large amounts of power associated with traveling waves at frequencies up to 0.1 day^{-1}. This band of frequencies also contains the three peaks identified earlier with an external and two internal normal modes. The question thus arises whether the presence of normal modes is necessary or sufficient to produce large enough traveling wave amplitudes for coherence between heat flux and temperature gradient to be realized. Some idea of the importance of normal modes can be gained by running the model as before, but with a slight change in the lower boundary condition that changes the phase speed of the external mode while leaving the phase speed of the internal modes unchanged. This can be done by forcing with the vertical velocity in pressure coordinates instead of the vertical velocity in geometric coordinates. Fig. 9 shows the squared coherence analysis for this run (curve B) compared to that for a run with the original lower boundary condition (curve A). The external mode, which was originally centered at a frequency of 0.09 day^{-1} is now located near 0.13 day^{-1}. We see that this has led to a drop in the coherence around 0.09 day^{-1} and to an increase at

0.13 day^{-1}. The latter increase, however, is barely sufficient to make the coherence significant at 0.13 day^{-1}. Apparently, the production of large oscillating heat fluxes by superposition of stationary and traveling waves depends not only on the existence of a normal mode, but also on the availability of sufficient forcing at the frequency of the mode. When the external mode is moved to 0.13 day^{-1}, the amount of power available to excite it is considerably less than when this mode was centered at 0.09 day^{-1} (Fig. 2). As a consequence, the eddy heat fluxes produced by the superposition of this mode and the stationary wave produce a signal which is just above the noise level.

An alternative way of testing the importance of normal modes is to run the model without an Ekman layer. Referring once again to Fig. 4, we note that, in the inviscid case, the power associated with all normal modes, but especially with the external mode, is increased. Fig. 10 shows the coherence for the inviscid case (curve B) compared to the coherence for the run with an Ekman layer. The increase in coherence over a band of frequencies centered on the frequency of the external mode (0.09 day^{-1}) is striking.

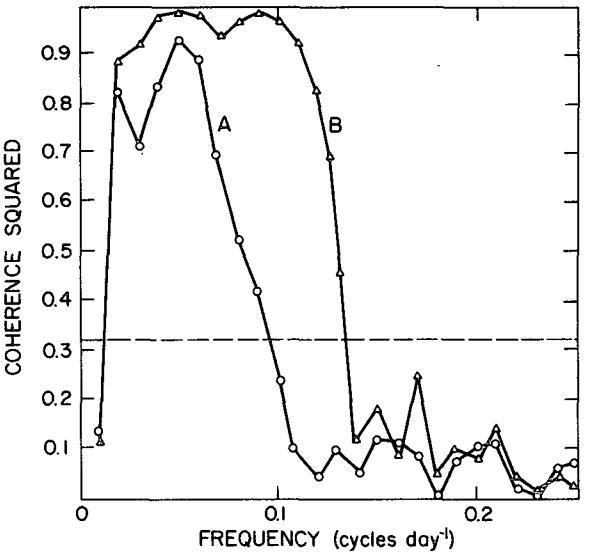

FIG. 10. Same as Fig. 9, except that curve (B) now shows the result of eliminating Ekman damping from (A).

4. Summary and conclusions

We have used a quasi-geostrophic β-plane model to investigate the response of the stratosphere to planetary waves forced stochastically at the ground. The forcing consists of a standing eddy vertical velocity field whose amplitude varies randomly about a time-average value. When the model is forced thus, quasi-regular oscillations are produced in eddy and mean fields at stratospheric levels.

We have applied the cross-spectrum analysis technique of Hayashi (1971) to the time-series of the eddy streamfunction and found that westward traveling waves are excited in the model. Large amounts of power are associated with these waves at frequencies up to 0.1 day^{-1} (Fig. 4). This band of frequencies also contains three peaks which correspond to an external and two internal normal modes. We conclude that oscillations in the eddy fields and, in particular, in the eddy heat flux produced by the model arise from the superposition of the traveling waves with the stationary wave maintained by the time-average forcing.

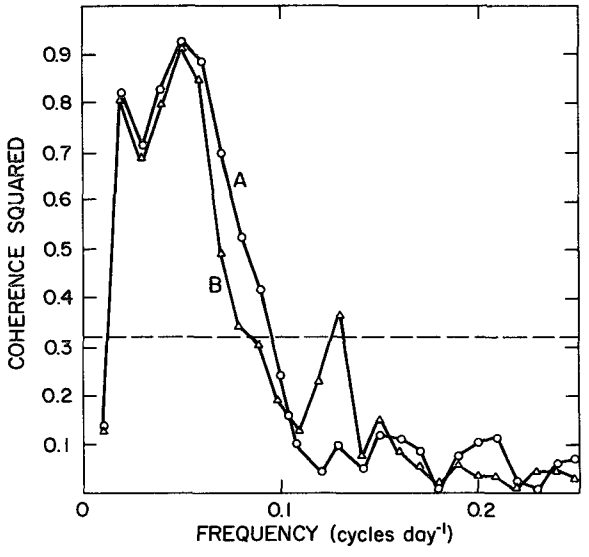

FIG. 9. Squared coherence between zonal mean temperature gradient and eddy heat flux for (A) the case with 5% noise added to the time series, and (B) the same case with the frequency of the external mode shifted to 0.13 day^{-1}.

Madden (1975) has argued that westward traveling waves with periods in the one to three week range force oscillations in the zonal mean temperature difference between high and middle latitudes in the stratosphere. Our results, shown in Fig. 7, resemble Madden's coherence analysis of observations in many important respects and lend support to his hypothesis. However, we have also shown that the presence of traveling waves is not in itself sufficient to produce coherence between eddy heat fluxes and the zonally averaged temperature gradient. By adding a prescribed amount of white noise to the model output, it becomes readily apparent that significant values of coherence occur only at frequencies where the signal in the time series of heat flux and temperature gradient is above the added noise. The addition of noise to the model output can be viewed as the counterpart of the uncertainty that accompanies the measurement of any quantity in the real atmosphere.

In our model, high coherences in the presence of added noise occur over a band of frequencies that corresponds roughly to those frequencies where substantial amounts of power are associated with traveling waves. As noted above, three peaks within this band can be identified with normal

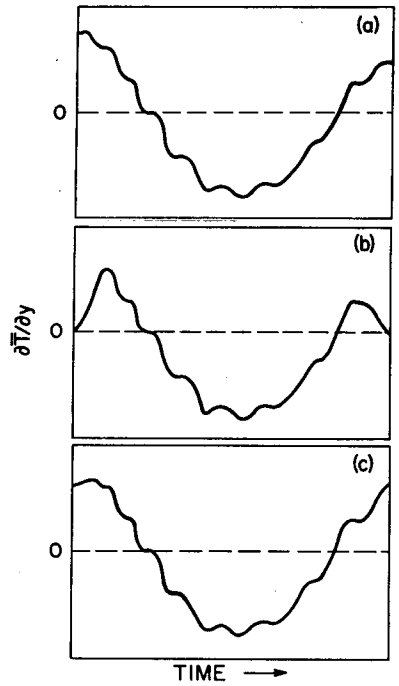

FIG. 11. Schematic illustration of two methods of tapering time series (a). In (b), the first and last 10% of (a) have been tapered to zero; in (c), tapering to the average value of the first and last members of (a) has been performed.

modes. The question then arises whether the presence of normal modes is necessary or sufficient to produce coherence. To gain some insight into this question, we performed two model runs wherein

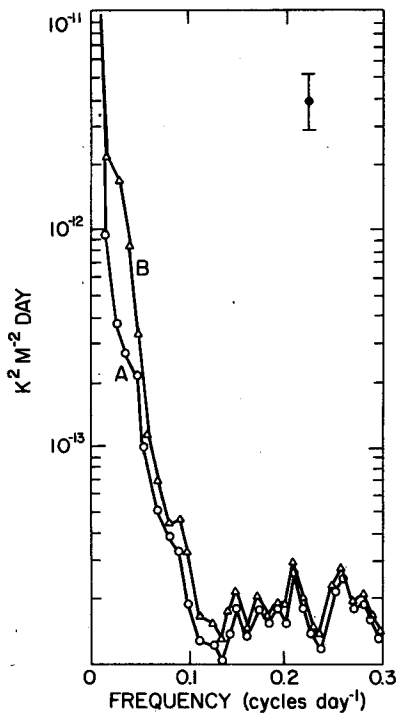

FIG. 12. Spectra of zonal mean temperature gradient obtained after (A) tapering to the average value of the first and last members of the time series, and (B) tapering to zero.

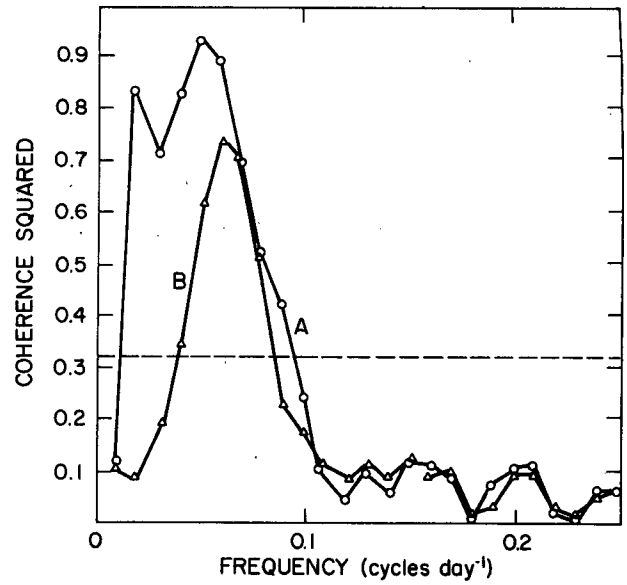

FIG. 13. The squared coherence computed for the two cases of Fig. 12.

the characteristics of the external mode were altered.

In the first of these runs, the lower boundary condition was modified in such a way that the frequency of the external mode increased from 0.09 to 0.13 day^{-1}. Under these circumstances, the coherence between heat flux and temperature gradient drops markedly at frequencies around 0.09 day^{-1} and increases near 0.13 day^{-1} (Fig. 9). However, the increase at 0.13 day^{-1} is barely sufficient to make the coherence there statistically significant. This is due to the fact that the amount of power available to excite the external mode is much less at 0.13 day^{-1} than at 0.09 day^{-1} (Fig. 2). We have also run the model without Ekman damping, having shown earlier that the amplitude of the external mode is much reduced by such dissipation. The squared coherence values computed from the inviscid case showed a remarkable increase about the frequency of the external mode (Fig. 10). From these runs we conclude that the external mode has considerable potential for generating eddy heat fluxes which are in turn able to force oscillations in the mean temperature gradient. However, enough power must be available at the frequency of the mode for the coherence between heat flux and temperature gradient to reach significant levels in the presence of noise.

Acknowledgment. The authors wish to thank Dr. Roland Madden for many helpful discussions during the course of this investigation.

APPENDIX

The Effect of Tapering on Spectral Estimates

A common procedure used in estimating the spectrum of a time series is to taper the first and

last 10% of the time series to zero after removing its mean and before using the fast Fourier transform to determine harmonic coefficients. Since, for the purpose of Fourier analysis, a time series of finite length is assumed to be one cycle of an infinite periodic series, tapering assures that no spurious high-frequency components will be introduced if the end points of the original time series have different values. However, this procedure can introduce its own kind of bias if the tapering operation results in significant modification of the time series.

Curve A in Fig. 11 is a schematic representation of the time series of zonal mean temperature gradient for one model season, after the time mean has been removed. Curve B shows the result of tapering the first and last 10% of A to zero. By contrast, curve C is obtained by tapering the first and last 10% of A to the average value of the first and last members of A. Clearly, for a series like A, the second method of tapering (which we have used in this paper) modifies the original time series to a much lesser extent than the traditional method.

In Fig. 12 we show spectra of the zonal mean temperature gradient estimated after tapering by each of the two methods mentioned above. Spectrum A corresponds to the tapering used in this paper, while spectrum B was obtained after tapering to zero. The variance of spectrum B has been increased significantly in the frequency range of $\sim 0.02-0.05$ day^{-1}.[3] This increased variance may be considered as noise and can be expected to have an effect on the coherence between time series whose spectra have been computed after tapering to zero. Fig. 13 shows squared coherences between mean temperature gradient and eddy heat flux. Curve A was obtained after tapering to the average of the first and last members of the time series. It represents the coherence obtained for one of the model runs discussed in the body of this paper. Curve B was obtained from exactly the same model output after tapering to zero. A drastic drop in coherence is evident in the 0.02–0.05 day^{-1} frequency range. This corresponds to the range of frequencies where bias is introduced into the spectral estimates by tapering the time series to zero.

Since some meteorological time series have a shape similar to curve A of Fig. 11, and since tapering to zero before performing harmonic analysis appears to be a fairly common procedure, it is possible that coherences between meteorological time series reported in the literature might have been underestimated in some cases. It may be worthwhile to repeat such calculations by a method that does not introduce the bias discussed here into the spectral estimates.

[3] It should be noted that the variance contained in spectrum A is nevertheless greater than that of spectrum B because tapering to zero reduces the overall variance more than tapering to the average of the endpoint values. However, this reduction takes place at very low frequencies (<0.01 day^{-1}) and is not readily apparent in Fig. 12.

REFERENCES

Dickinson, R. E., 1973: Method of parameterization for infrared cooling between altitudes of 30 and 70 km. *J. Geophys. Res.*, **78**, 4451–4457.

Finger, F. G., H. M. Woolf and C. E. Anderson, 1966: Synoptic analyses of the 5-, 2-, and 0.4-millibar surfaces for the IQSY period. *Mon. Wea. Rev.*, **94**, 651–661.

Geisler, J. E., and R. E. Dickinson, 1975: External Rossby modes on a β-plane with realistic vertical wind shear. *J. Atmos. Sci.*, **32**, 2082–2093.

——, and ——, 1976: The five-day wave on a sphere with realistic zonal winds. *J. Atmos. Sci.*, **33**, 632–641.

Gilman, D. L., F. J. Fuglister and J. M. Mitchell, 1963: On the power spectrum of "red noise." *J. Atmos. Sci.*, **20**, 182–184.

Harwood, R. S., 1975: The temperature structure of the Southern Hemisphere stratosphere August–October 1971. *Quart. J. Roy. Meteor. Soc.*, **101**, 75–91.

Hayashi, Y., 1971: A generalized method of resolving disturbances into progressive and retrogressive waves by space Fourier and time cross-spectral analyses. *J. Meteor. Soc. Japan*, **49**, 125–128.

Hirota, I., 1971: Excitation of planetary Rossby waves in the winter stratosphere by periodic forcing. *J. Meteor. Soc. Japan*, **49**, 439–448.

——, and Y. Sato, 1969: Periodic variations of the winter stratospheric circulation and intermittent vertical propagation of planetary waves. *J. Meteor. Soc. Japan*, **47**, 390–402.

Holton, J. R., and C. Mass, 1976: Stratospheric vacillation cycles. *J. Atmos. Sci.*, **33**, 2218–2225.

——, and T. Dunkerton, 1978: On the role of wave transience and dissipation in stratospheric mean flow vacillations. *J. Atmos. Sci.*, **35**, 740–744.

Jenkins, G. M., and D. G. Watts, 1968: *Spectral Analysis and Its Applications*. Holden-Day, 525 pp.

Julian, P. R., 1975: Comments on the determination of significance levels of the coherence statistic. *J. Atmos. Sci.*, **32**, 836–837.

Leovy, C. B., and P. J. Webster, 1976: Stratospheric long waves: Comparison of thermal structure in the Northern and Southern Hemispheres. *J. Atmos. Sci.*, **33**, 1624–1638.

Madden, R. A., 1975: Oscillations in the winter stratosphere: Part 2. The role of horizontal heat transports and the interaction of transient and stationary planetary waves. *Mon. Wea. Rev.*, **103**, 717–729.

——, 1978: Further evidence of traveling planetary waves. *J. Atmos. Sci.*, **35**, 1605–1618.

McIntyre, M. E., 1980: An introduction to the generalized Lagrangian-mean description of wave, mean-flow interaction. *Pure Appl. Geophys.*, **118**, 152–176.

Miller, A. J., 1974: Periodic variation of atmospheric circulation at 14–16 days. *J. Atmos. Sci.*, **31**, 720–726.

Muench, H. S., 1965: On the dynamics of the wintertime stratosphere circulation. *J. Atmos. Sci.*, **22**, 349–360.

Salby, M. L., 1981: Rossby normal modes in nonuniform background configurations. Part II: Equinox and solstice conditions. *J. Atmos. Sci.*, **38**, 1827–1840.

Schoeberl, M. R., and J. H. E. Clark, 1980: Resonant planetary waves in a spherical atmosphere. *J. Atmos. Sci.*, **37**, 20–28.

van Loon, H., R. A. Madden and R. L. Jenne, 1975: Oscillations in the winter stratosphere: Part 1. Description. *Mon. Wea. Rev.*, **103**, 154–162.

Webster, P. J., and J. L. Keller, 1975: Atmospheric variations: Vacillations and index cycles. *J. Atmos. Sci.*, **32**, 1283–1300.